

# PR Current Control with Harmonic Compensation in Grid Connected PV Inverters

Daniel Zammit, Cyril Spiteri Staines, Maurice Apap

**Abstract**—This paper presents a study on Proportional Resonant (PR) current control with additional PR harmonic compensators for Grid Connected Photovoltaic (PV) Inverters. Both simulation and experimental results will be presented. Testing was carried out on a 3kW Grid-Connected PV Inverter which was designed and constructed for this research.

**Keywords**—Inverters, Proportional-Resonant Controllers, Harmonic Compensation, Photovoltaic.

## I. INTRODUCTION

GRID-CONNECTED PV Inverter systems have become an important power generating method and the number of these systems connected to the grid is always increasing. Therefore it is important to control the harmonics generated by these inverters to limit their adverse effects on the grid power quality. The harmonic limits are set in IEEE and European IEC standards (IEEE 929, IEEE 1547 and IEC 61727) which suggest limits for the current total harmonic distortion (THD) factor and also for the magnitude of each harmonic.

The current controller can have a significant effect on the quality of the current supplied to the grid by the PV inverter, and therefore it is important that the controller provides a high quality sinusoidal output with minimal distortion to avoid creating harmonics. A commonly used current controller for grid-connected PV inverters is the PR current controller. This controller is highly suited to operate with sinusoidal references like the reference used in grid-connected PV inverters, thus making it an optimal solution for this application. The PR controller provides gain at a certain frequency (resonant frequency) and almost no gain exists at the other frequencies.

The PR current controller is presented and discussed in [1]-[3]. Although this controller has a high ability to track a sinusoidal reference such as a current waveform, the output current of the grid-connected inverter is not immune from any harmonic content [4]. Harmonics in the output current can result due to electronic component non-linearities within the inverter itself as well as from harmonics which are already present in the grid. Selective harmonics in the current can be compensated by using additional PR controllers which act at particular harmonic frequencies to be reduced or eliminated such as the 3<sup>rd</sup>, 5<sup>th</sup>, 7<sup>th</sup> and so on. This compensation can be used to reduce the current THD and make the inverter compliant to the IEEE and IEC standards [1], [5], [6].

Mr Daniel Zammit, Prof. Cyril Spiteri Staines, and Dr Maurice Apap are with the Department of Industrial Electrical Power Conversion, University of Malta, Msida, MSD 2080 (e-mail: daniel.zammit@um.edu.mt, cyril.spiteri-staines@um.edu.mt, maurice.apap@um.edu.mt).

This paper presents the design of a single phase 3kW grid-connected PV inverter, which includes the design of the LCL filter and the current control. A comparison between PR current control on its own and with additional harmonic compensators as used in grid-connected PV inverters is also presented, both by simulations and by experimental tests. Selective harmonic compensation was applied for the 3<sup>rd</sup>, 5<sup>th</sup> and 7<sup>th</sup> harmonics.

Fig. 1 shows a block diagram of the Grid-Connected PV Inverter system connected to the grid through an LCL filter.

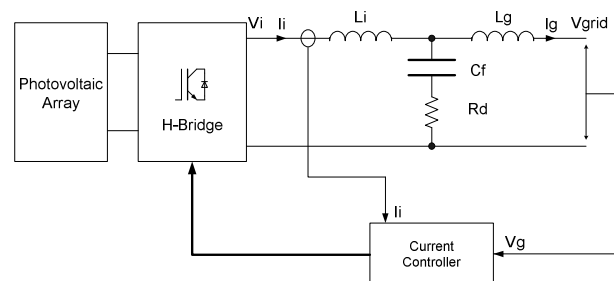


Fig. 1 Block diagram of the Grid-Connected PV Inverter with the LCL Filter

## II. LCL FILTER AND CURRENT CONTROL

### A. LCL Filter

The transfer function of the LCL filter in terms of the inverter current  $I_i$  and the inverter voltage  $U_i$ , neglecting  $R_d$ , is:

$$G_F(s) = \frac{I_i}{U_i} = \frac{1}{L_i s} \frac{(s^2 + [\frac{1}{L_g C_f}])}{(s^2 + [(L_i + L_g) / (L_i L_g C_f)])} \quad (1)$$

where,  $L_i$  is the inverter side inductor

$L_g$  is the grid side inductor

and  $C_f$  is the filter capacitor

The resonant frequency of the filter is given by:

$$\omega_{res} = \sqrt{\frac{(L_i + L_g)}{(L_i L_g C_f)}} \quad (2)$$

The transfer function in (1) does not include the damping resistor  $R_d$ . The introduction of  $R_d$  in series with the capacitor  $C_f$  increases stability and reduces resonance [7]. This method of damping is a type of Passive Damping. Whilst there exist other methods of passive damping and also more advanced Active Damping methods, this particular damping method

used was considered enough for the aim and purpose of comparing the two current controllers due to its simplicity. The transfer function of the filter taking in consideration the damping resistor  $R_d$  is:

$$G_F(s) = \frac{I_i}{U_i} = \frac{1}{L_i s} \frac{(s^2 + s(\frac{R_d}{L_g}) + [1/L_g C_f])}{(s^2 + s[(L_i + L_g)R_d]/L_i L_g + [(L_i + L_g)/(L_i L_g C_f)])} \quad (3)$$

### B. PR Control

Fig. 2 shows the PR current control strategy.  $I_i$  is the inverter output current,  $I_i^*$  is the inverter current reference and  $U_i^*$  is the inverter voltage reference.

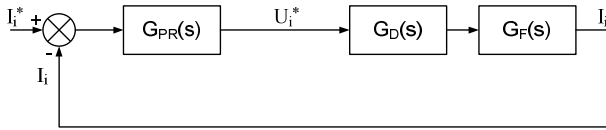


Fig. 2 The PR Current Control

The PR current controller  $G_{PR}(s)$  is represented by:

$$G_{PR}(s) = K_P + K_I \frac{s}{s^2 + \omega_0^2} \quad (4)$$

where,  $K_P$  is the Proportional Gain term,  $K_I$  is the Integral Gain term and  $\omega_0$  is the resonant frequency.

$G_F(s)$  represents the LCL filter.  $G_D(s)$  represents the processing delay of the microcontroller, which is typically equal to the time of one sample  $T_s$  and is represented by:

$$G_D(s) = \frac{1}{1 + sT_s} \quad (5)$$

The ideal resonant term on its own in the PR controller provides an infinite gain at the ac frequency  $\omega_0$  and no phase shift and gain at the other frequencies [8]. The  $K_P$  term determines the dynamics of the system; bandwidth, phase and gain margins [8].

Equation (4) represents an ideal PR controller which can give stability problems because of the infinite gain. To avoid these problems, the PR controller can be made non-ideal by introducing damping as shown in (6):

$$G_{PR}(s) = K_P + K_I \frac{2\omega_c s}{s^2 + 2\omega_c s + \omega_0^2} \quad (6)$$

where,  $\omega_c$  is the bandwidth around the ac frequency of  $\omega_0$ .

With (6) the gain of the PR controller at the ac frequency  $\omega_0$  is now finite but it is still large enough to provide only a very small steady state error. This equation also makes the controller more easily realizable in digital systems due to their finite precision [9].

### C. PR Control with Harmonic Compensators

Fig. 3 shows the PR current control with additional harmonic compensation strategy.

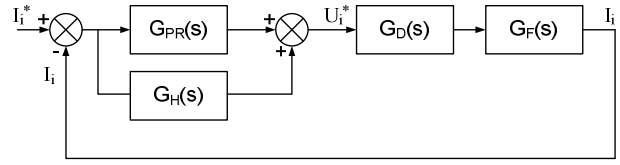


Fig. 3 The PR Current Control with Harmonic Compensators

The harmonic compensator  $G_H(s)$  is represented by:

$$G_H(s) = \sum_{h=3,5,7,\dots} K_{Ih} \frac{s}{s^2 + (h\omega_0)^2} \quad (7)$$

where,  $K_{Ih}$  is the Resonant term at the particular harmonic and  $h\omega_0$  is the resonant frequency of the particular harmonic.

The harmonic compensator for each harmonic frequency is added to the fundamental frequency PR controller to form the complete current controller, as shown in Fig. 3.

Equation (7) represents an ideal harmonic compensator which as stated for the fundamental PR controller, can give stability problems due to the infinite gain. To avoid these problems, the harmonic compensator equation can be made non-ideal by representing it using (8):

$$G_H(s) = \sum_{h=3,5,7,\dots} K_{Ih} \frac{2\omega_c s}{s^2 + 2\omega_c s + (h\omega_0)^2} \quad (8)$$

where,  $\omega_c$  is the bandwidth around the particular harmonic frequency of  $h\omega_0$ .

As for the case of the fundamental PR controller, with (8) the gain of the harmonic compensator at the harmonic frequency  $h\omega_0$  is now finite but it is still large enough to provide compensation.

## III. LCL FILTER DESIGN

To carry out the tests using the PR current control without and with harmonic compensation, a 3kW Grid-Connected Inverter including the LCL filter was designed and constructed. The LCL filter was designed following the procedure in [8] and [10]. Designing for a dc-link voltage of 358V, maximum ripple current of 20% of the grid peak current, a switching frequency of 10kHz, filter cut-off frequency of 2kHz and the capacitive reactive power not exceeding 5% of rated power, the following values of the LCL filter were obtained:  $L_i = 1.2\text{mH}$ ,  $L_g = 0.7\text{mH}$ ,  $C_f = 9\mu\text{F}$  and  $R_d = 8\Omega$ .

## IV. PR CONTROLLER AND HARMONIC COMPENSATORS DESIGN

### A. PR Controller Design

The PR controller was designed for a resonant frequency  $\omega_0$  of 314.16rad/s (50Hz) and  $\omega_c$  was set to be 0.5rad/s, obtaining

a  $K_p$  of 6.8 and  $K_i$  of 1498.72.

Fig. 4 shows the root locus plot in Matlab of the system including the LCL filter, the processing delay, anti-aliasing filter in the output current feedback path and the PR controller. The root locus plot shows that the designed system is stable.

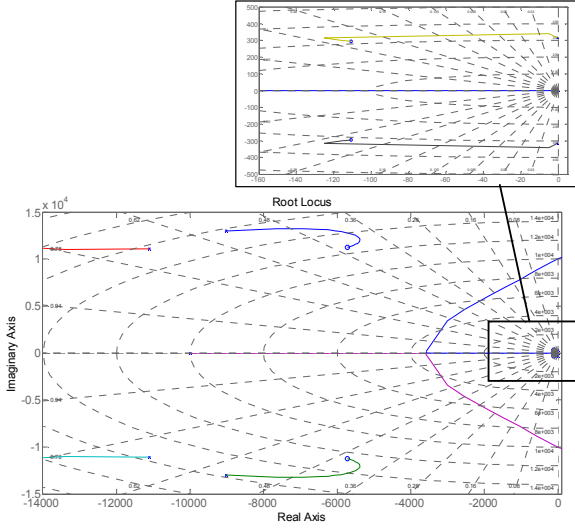


Fig. 4 Root Locus of the Inverter with the PR Controller

Figs. 5 and 6 show the open loop bode diagram and the closed loop bode diagram of the system, respectively. From the open loop bode diagram, the Gain Margin obtained is 13.9dB at a frequency of 9970rad/s and the Phase Margin obtained is 51deg at a frequency of 3300rad/s.

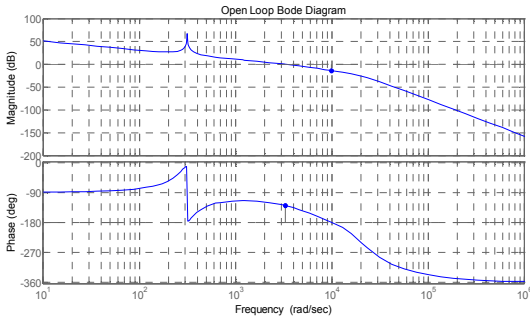


Fig. 5 Open Loop Bode Diagram of the System with PR Control

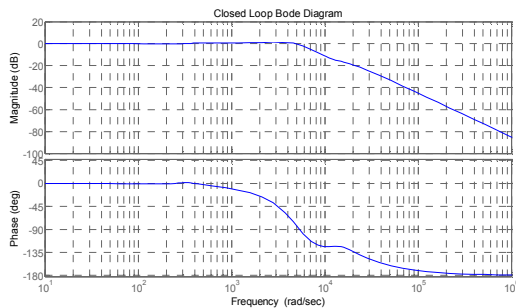


Fig. 6 Closed Loop Bode Diagram of the System with PR Control

### B. Harmonic Compensators Design

Additional harmonic compensators were designed for the 3<sup>rd</sup>, 5<sup>th</sup> and 7<sup>th</sup> harmonics. The 3<sup>rd</sup> harmonic compensator at a resonant frequency  $3\omega_0$  of 942.48rad/s (150Hz) was designed with a  $\omega_c$  of 2.5rad/s and a  $K_i$  of 211.208. The 5<sup>th</sup> harmonic compensator at a resonant frequency  $5\omega_0$  of 1570.8rad/s (250Hz) was designed with a  $\omega_c$  of 4.5rad/s and a  $K_i$  of 83.867. The 7<sup>th</sup> harmonic compensator at a resonant frequency  $7\omega_0$  of 2199.11rad/s (350Hz) was designed with a  $\omega_c$  of 10rad/s and a  $K_i$  of 40.834.

Fig. 7 shows the root locus plot in Matlab of the system with the additional harmonic compensators. The root locus plot shows that the designed system is stable.

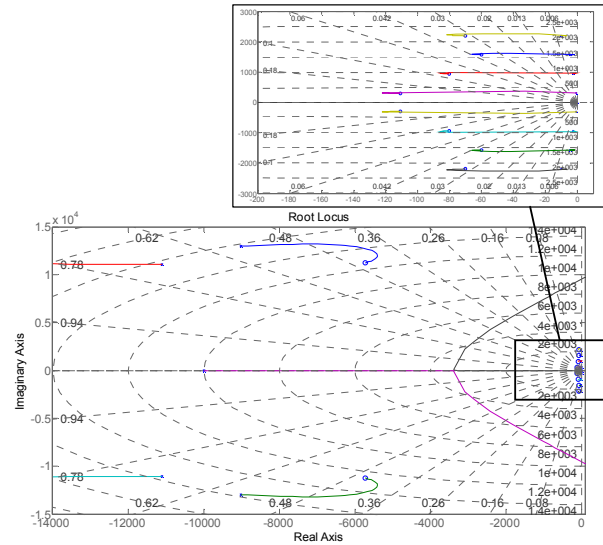


Fig. 7 Root Locus of the Inverter with the Fundamental PR Controller and the Harmonic Compensators

Figs. 8 and 9 show the open loop bode diagram and the closed loop bode diagram of the system, respectively. From the open loop bode diagram, the Gain Margin obtained is 13.2dB at a frequency of 9520rad/s and the Phase Margin obtained is 41.8deg at a frequency of 3310rad/s.

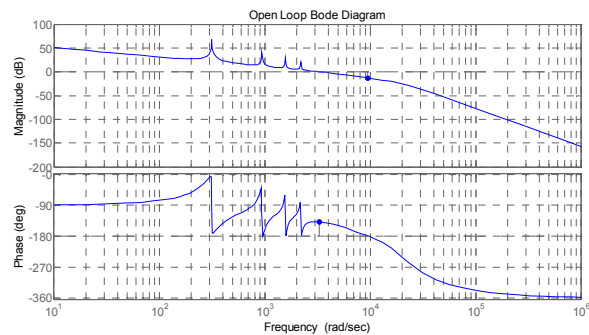


Fig. 8 Open Loop Bode Diagram of the System with the Fundamental PR Controller and the Harmonic Compensators

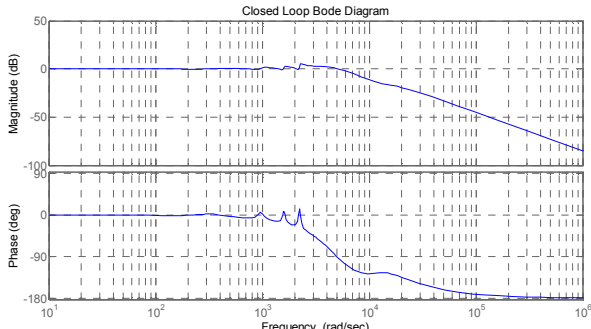


Fig. 9 Closed Loop Bode Diagram of the System with the Fundamental PR Controller and the Harmonic Compensators

V. SIMULATIONS

The 3kW Grid-Connected PV Inverter was modeled and simulated in Simulink with PLECS blocksets. The grid voltage was set to 325V peak (230V rms), the dc-link voltage was set to 360V and the reference current was set to 18.446A peak to simulate a 3kW inverter. 3<sup>rd</sup>, 5<sup>th</sup> and 7<sup>th</sup> harmonics were added to the grid voltage with amplitudes of 10V, 4V and 2V, respectively, which correspond to 3.077%, 1.231% and 0.615% of the grid voltage, to distort the grid voltage sinusoidal waveform. Simulations were carried out to observe the effect of the harmonics with and without harmonic compensation on the inverter voltage and grid current.

Figs. 10 and 11 show the inverter voltage ( $V_{pwm}$ ), the grid voltage ( $V_{grid}$ ), the capacitor voltage ( $V_{cap}$ ), the inverter current ( $I_{inv}$ ), the grid current ( $I_{grid}$ ) and the reference current ( $I_{ref}$ ) from the simulation in the s-domain using the PR controller without and with harmonic compensation, respectively.

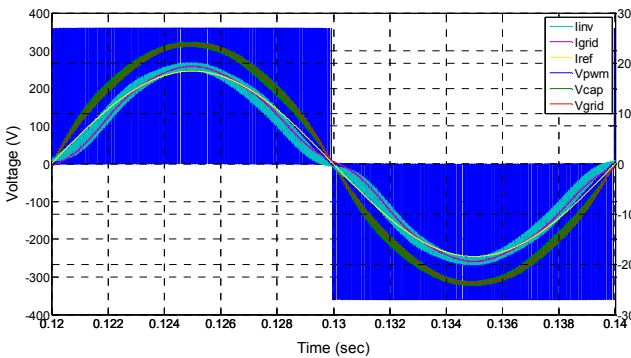


Fig. 10 Simulation Result from the Inverter with PR Current Control without Harmonic Compensation

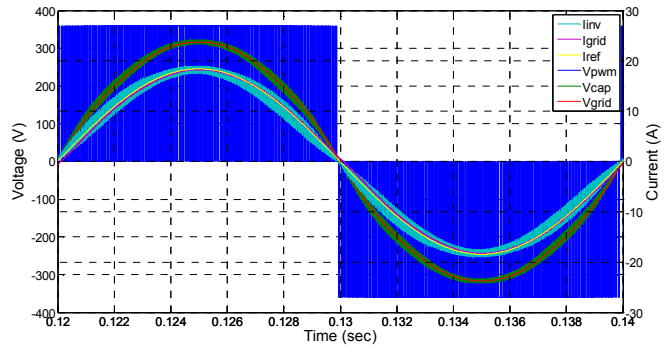


Fig. 11 Simulation Result from the Inverter with PR Current Control with Harmonic Compensation

Figs. 12 and 13 show the harmonic spectrum of the grid current from the simulation in the s-domain using the PR controller without and with harmonic compensation, respectively.

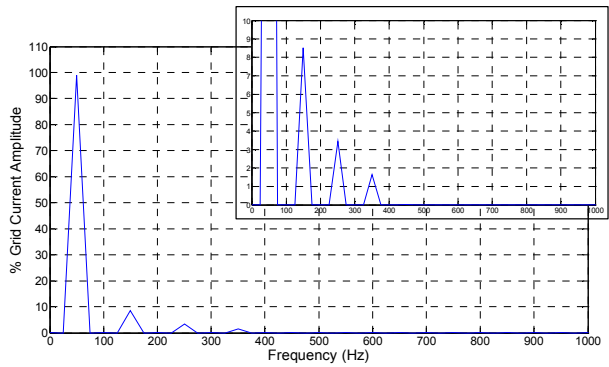


Fig. 12 Harmonic Spectrum of the Grid Current from the Simulation with PR Current Control without Harmonic Compensation

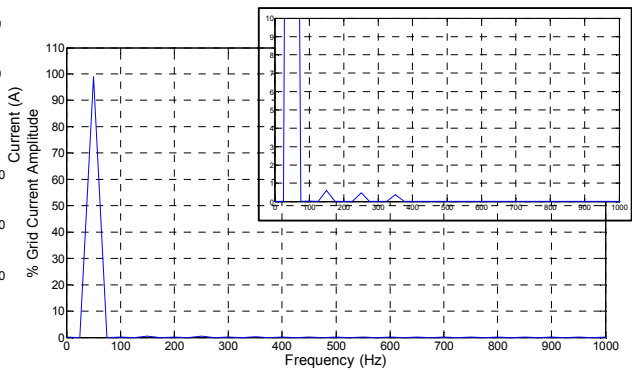


Fig. 13 Harmonic Spectrum of the Grid Current from the Simulation with PR Current Control with Harmonic Compensation

From the s-domain simulation results without harmonic compensation shown in Figs. 10 and 12 the grid current  $I_{grid}$  was highly affected by the harmonics present in the grid voltage. When considering the harmonics of the grid current as a percentage of the reference current the 3<sup>rd</sup>, 5<sup>th</sup> and 7<sup>th</sup> harmonics were about 8.528%, 3.44% and 1.649%, respectively. When the harmonic compensators were applied

the 3<sup>rd</sup>, 5<sup>th</sup> and 7<sup>th</sup> harmonics in the grid current  $I_{grid}$  were reduced to 0.613%, 0.474% and 0.388%, respectively, as can be observed from the simulation results shown in Figs. 11 and 13. Simulations in the z-domain provided similar results as those in the s-domain.

VI. GRID-CONNECTED PV INVERTER TESTING

The constructed 3kW Grid-Connected PV Inverter test rig is shown in Fig. 14. The inverter was operated at a switching frequency of 10kHz and was connected to a 50Hz grid supply. The inverter was controlled by the dsPIC30F4011 microcontroller from Microchip. Testing was carried out using the PR controller without and with the selective harmonic compensators to analyze the performance of the compensators. The inverter was connected to the grid using a variac to allow variation of the grid voltage for testing purposes. The dc link voltage was obtained from a dc power supply.

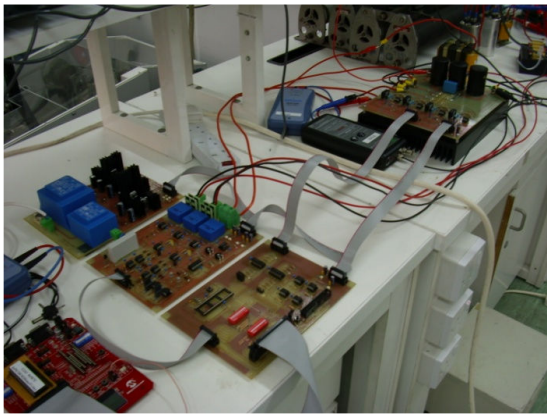


Fig. 14 3kW Grid-Connected PV Inverter Test Rig

Tests were performed to measure the voltage harmonics present in the grid voltage. The 3<sup>rd</sup>, 5<sup>th</sup> and 7<sup>th</sup> harmonics present in the grid voltage were typically about 0.9%, 1.912% and 0.231%, respectively.

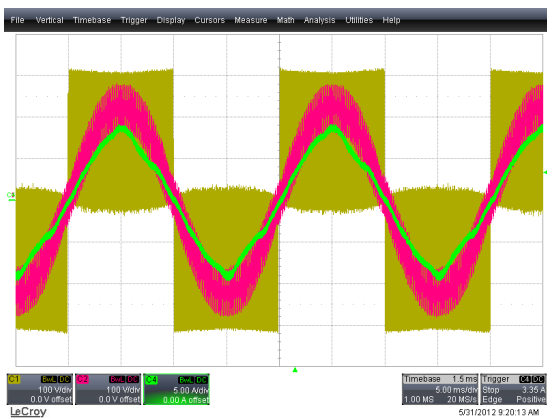


Fig. 15 Inverter Output Voltage (Gold/Yellow Trace), Grid Voltage (Violet Trace) and Grid Current (Green Trace) with a Preset Current of 8A Peak using the PR Controller without Harmonic Compensation

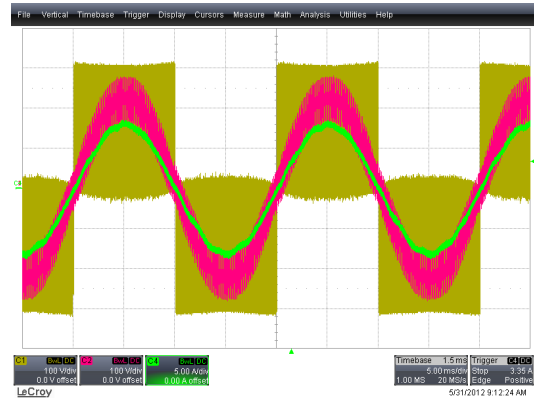


Fig. 16 Inverter Output Voltage (Gold/Yellow Trace), Grid Voltage (Violet Trace), and Grid Current (Green Trace) with a Preset Current of 8A Peak using the PR Controller with 3<sup>rd</sup>, 5<sup>th</sup> and 7<sup>th</sup> Harmonic Compensation

Figs. 15 and 16 show the inverter output voltage, the grid voltage and the grid current for a dc-link voltage of 300V, a grid voltage of 154V and a preset reference value of 8A peak using the PR controller without and with harmonic compensation, respectively.

Figs. 17 and 18 show the grid current for the grid-connected inverter with the PR current controller without and with harmonic compensation, respectively.  $I_g$  is the grid current,  $I_{gr}$  is the reconstructed grid current up to its 13<sup>th</sup> harmonic (a reconstruction of the grid current by adding the first 13 lower harmonics) and  $I_{gfund}$  is the fundamental component of the grid current.

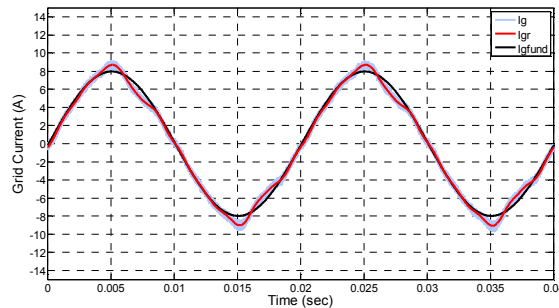


Fig. 17 Grid Current with PR Current Control without Harmonic Compensation

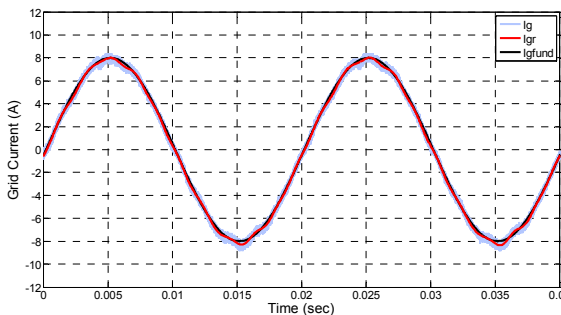


Fig. 18 Grid Current with PR Current Control and the 3<sup>rd</sup>, 5<sup>th</sup> and 7<sup>th</sup> Harmonic Compensators

Figs. 19 and 20 show the harmonic spectrum of the grid current with PR current control without and with harmonic compensation, respectively. Without harmonic compensation the 3<sup>rd</sup>, 5<sup>th</sup> and 7<sup>th</sup> harmonics resulted about 5.574%, 4.231% and 2.435% of the reference value of 8A peak, respectively. When the harmonic compensators were used the 3<sup>rd</sup>, 5<sup>th</sup> and 7<sup>th</sup> harmonics resulted about 0.378%, 0.641% and 0.24% of the reference value of 8A peak, respectively.

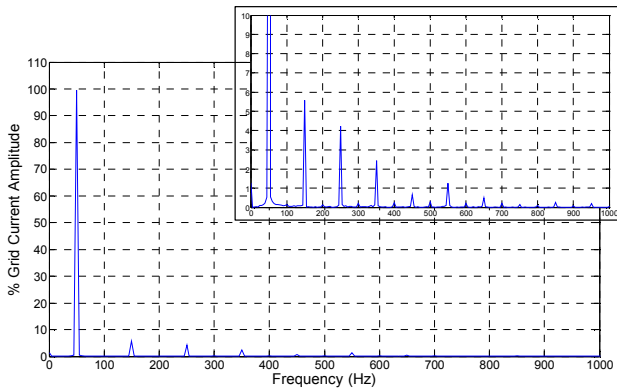


Fig. 19 Harmonic Spectrum of the Grid Current with PR Current Control without Harmonic Compensation

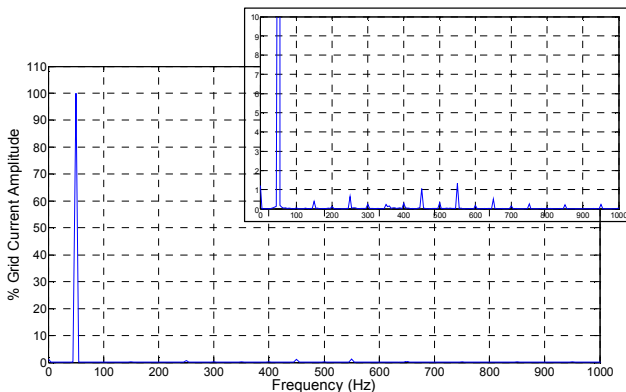


Fig. 20 Harmonic Spectrum of the Grid Current with PR Current Control and the 3<sup>rd</sup>, 5<sup>th</sup> and 7<sup>th</sup> Harmonic Compensators

## VII. COMPARISON OF EXPERIMENTAL RESULTS

TABLE I  
FUNDAMENTAL AND HARMONICS FOR THE PR CURRENT CONTROLLED GRID-CONNECTED INVERTER WITH SELECTIVE HARMONIC COMPENSATION

	Fundamental	3 <sup>th</sup> Harm	5 <sup>th</sup> Harm	7 <sup>th</sup> Harm
	$I_g$	$I_g$	$I_g$	$I_g$
Fundamental PR only	100 %	5.574 %	4.231 %	2.435 %
Fund PR 3 <sup>rd</sup> , 5 <sup>th</sup> , 7 <sup>th</sup>	100 %	0.378 %	0.641 %	0.24 %
H. Comp				

The 3<sup>rd</sup>, 5<sup>th</sup> and 7<sup>th</sup> harmonics present in the grid voltage were typically about 0.9%, 1.912% and 0.231%, respectively. Table I shows the percentage fundamental and harmonic content of the grid current for the PR current controlled grid-connected inverter without and with the selective harmonic

compensators. The percentage calculations for the grid current are based on the reference current of 8A peak. As can be observed from the experimental results above, the harmonic compensators have drastically reduced the 3<sup>rd</sup>, 5<sup>th</sup> and 7<sup>th</sup> harmonics in the grid current. This agrees with the results obtained in the simulations.

These harmonics would be reduced further if the gain of the harmonic compensators at the harmonic frequency is increased, but this could possibly cause the system to go unstable. This would happen because by increasing the gain, the phase peaks at the harmonic frequencies would also increase which would cut the  $-180^\circ$  line providing a negative gain margin that drives the system unstable. As can be observed from the open loop bode diagram in Fig. 8 the phase peaks are already at the maximum possible. A possible solution might be to increase the bandwidth of the system by increasing the proportional gain  $K_p$  of the fundamental PR controller which would make room for larger gains for the harmonic compensators. But by increasing the bandwidth of the system the chance of being affected by higher harmonics (9<sup>th</sup>, 11<sup>th</sup> and 13<sup>th</sup> and so on) is increased which would lead to the need of additional harmonic compensators on those harmonics too. Therefore a compromise has to be found, to obtain the lowest harmonics possible with also the narrowest bandwidth possible.

The IEEE 929 and IEEE 1547 standards allow a limit of 4% for each harmonic from 3<sup>rd</sup> to 9<sup>th</sup> and 2% for 11<sup>th</sup> to 15<sup>th</sup> [11], [12]. The IEC 61727 standard specifies similar limits [13]. As can be observed from the results obtained the 3<sup>rd</sup> and 5<sup>th</sup> harmonics were above the limit when no harmonic compensation was applied. These harmonics result from the inverter itself due to the non-linearities in the inverter and also from the harmonics already present in the grid supply. The harmonic compensators reduced the 3<sup>rd</sup> and 5<sup>th</sup> harmonics within the limits and reduced further the 7<sup>th</sup> harmonic, thus making the inverter compliant to the standard regulations.

## VIII. CONCLUSION

This paper has presented a study on Proportional Resonant (PR) current control with additional PR harmonic compensators for Grid Connected Photovoltaic (PV) Inverters. A 3kW grid connected PV inverter was designed and built for this research. This paper covered the design of the LCL filter, the PR control and also the design of the selective harmonic compensators for the 3<sup>rd</sup>, 5<sup>th</sup> and 7<sup>th</sup> harmonics. Results from simulations and experimental analysis of a 3kW inverter connected to the 50Hz grid are shown. Both simulation and experimental results show the effectiveness of the harmonic compensators to reduce the harmonics in the grid current. The 3<sup>rd</sup>, 5<sup>th</sup> and 7<sup>th</sup> harmonics in the grid current were reduced from about 5.574%, 4.231% and 2.435%, respectively, to about 0.378%, 0.641% and 0.24%, respectively. The 3<sup>rd</sup>, 5<sup>th</sup> and 7<sup>th</sup> harmonics present in the grid voltage were typically about 0.9%, 1.912% and 0.231%, respectively. This reduction in harmonics made the grid connected inverter compliant to the standard regulations.

## REFERENCES

- [1] R. Teodorescu, F. Blaabjerg, U. Borup, M. Liserre, "A New Control Structure for Grid-Connected LCL PV Inverters with Zero Steady-State Error and Selective Harmonic Compensation", APEC'04 Nineteenth Annual IEEE Conference, California, 2004.
- [2] M. Liserre, R. Teodorescu, Z. Chen, "Grid Converters and their Control in Distributed Power Generation Systems", IECON 2005 Tutorial, 2005.
- [3] M. Ciobotaru, R. Teodorescu, F. Blaabjerg, "Control of a Single-Phase PV Inverter", EPE2005, Dresden, 2005.
- [4] D. Zammit, C. Spiteri Staines, M. Apap, "Comparison between PI and PR Current Controllers in Grid Connected PV Inverters", WASET, International Journal of Electrical, Electronic Science and Engineering, Vol. 8, No. 2, 2014
- [5] R. Teodorescu, F. Blaabjerg, M. Liserre, P. C. Loh, "Proportional-Resonant Controllers and Filters for Grid-Connected Voltage-Source Converters", IEEE Proc. Electr. Power Appl, Vol. 153, No. 5, 2006.
- [6] M. Castilla, J. Miret, J. Matas, L. G. de Vicuna, J. M. Guerrero, "Control Design Guidelines for Single-Phase Grid-Connected Photovoltaic Inverters with Damped Resonant Harmonic Compensators", IEEE Transactions on Industrial Power Electronics, Vol. 56, No. 11, 2009.
- [7] V. Pradeep, A. Kolwalkar, R. Teichmann, "Optimized Filter Design for IEEE 519 Compliant Grid Connected Inverters", IICPE 2004, Mumbai, India, 2004.
- [8] R. Teodorescu, M. Liserre, P. Rodriguez, "Grid Converters for Photovoltaic and Wind Power Systems", Wiley, 2011.
- [9] D. N. Zmood, D. G. Holmes, "Stationary Frame Current Regulation of PWM Inverters with Zero Steady-State Error", IEEE Transactions on Power Electronics, Vol. 18, No. 3, May 2003.
- [10] M. Liserre, F. Blaabjerg, S. Hansen, "Design and Control of an LCL-Filter Based Three Phase Active Rectifier", IEEE Transactions on Industry Applications, Vol 41, No. 5, Sept/Oct 2005.
- [11] IEEE 929 2000 Recommended Practice for Utility Interface of Photovoltaic (PV) Systems.
- [12] IEEE 1547 Standard for Interconnecting Distributed Resources with Electric Power Systems.
- [13] IEC 61727 2004 Standard Photovoltaic (PV) Systems – Characteristics of the Utility Interface.